Applied Physics A (2020) 126:490
https://doi.org/10.1007/s00339-020-03668-2

Applied Physics A
Materials Science & Processing

S.I. : CURRENT STATE-OF-THE-ART IN LASER ABLATION

Laser welding of highly reflective metal with absorbance-enhanced surface structure fabricated using picosecond laser

Tetsuo Sakai[1] · **Masatoshi Hirono**[1]

Received: 16 October 2019 / Accepted: 26 May 2020 / Published online: 5 June 2020

Abstract
We present a method to stably weld a copper at lower laser power by blackening the surface. Since the reflectivity of copper is approximately 97% in the infrared range, a precise and stable processing of copper is difficult even at high power using infrared laser. To decrease the reflectivity, we fabricated light-absorbing nano-structure on copper surface using picosecond laser pulses. The structure consists of aggregations of nano-particles, and is capable of absorbing as much as 80% of incident light. We demonstrated that a copper with this structure can be welded using 70% lower irradiation power than a copper without it. Additionally, we theoretically investigated the light-absorbing nano-structure using 3D finite-difference time-domain (FDTD) method.

Keywords Laser ablation · Copper · Nano-structure · Absorbance-enhanced surface structure · Picosecond laser · Femtosecond laser · Ultrashort pulse laser

1 Introduction

Laser welding has become popular in manufacturing process for mass production since the appearance of high-power CW infrared lasers [1–3]. In recent years, high-speed laser welding using galvanometer optical scanner is possible even for material with reflectivity as much as aluminum [4]. Since this welding method enables precise processing [4], it has shown to be effective in welding fine aluminum structure like a lithium ion battery [5]. However, in case of copper, which not only has high reflectivity but also high melting point and high thermal conductivity, a precise and stable welding process is difficult. To stabilize a welded state, various studies have been done such as laser power modulation [6] and harmonic beam combination [7]. Recently, CW Nd:YAG SHG laser and blue laser diode have been developed for a stable processing of copper due to its high absorbance at shorter wavelength [8, 9]. The process using a short wavelength is simple and manageable, but their laser power is still insufficient to weld at high speed.

We focused on a method to increase absorbance without using short wavelength laser. The method is a blackening of material surface by ultra-short pulse laser processing [10–15]. Such surface blackening had been studied to increase opto-electron conversion efficiency of silicon [16]. Vorobyev and Guo investigated the fabrication method using femtosecond laser pulse and controlled a color of various kinds of metal surfaces [11–13]. Recently, a potential to increase fabrication efficiency of the blackened surface using femtosecond fiber laser and picosecond laser at high repetition rate was reported [14, 15]. Here we studied the blackening of copper surface by picosecond laser processing, and we demonstrated a laser welding of the blackened copper surface at lower power compared to non-blackened surface. We also theoretically investigated a principle of the increased absorbance using the 3D finite-difference time-domain (FDTD) method.

2 Optical properties of blackened copper surface

2.1 Experimental procedure

The experiments were performed using a picosecond laser (Talisker Ultra 355–4, COHERENT Inc.). The laser output

✉ Tetsuo Sakai
tetsuo.sakai@toshiba.co.jp

[1] Corporate Manufacturing Engineering Center, Toshiba Corporation, 33, Shin-Isogo-Cho, Isogo-ku, Yokohama 235-0017, Japan

13 ps duration pulses at center wavelength of 532 nm (SHG) with maximum power of 7.45 W and maximum repetition rate of 200 kHz. In the experiment, a copper substrate ($50\times100\times5$ mm^3, oxygen-free copper) was placed in chamber as shown Fig. 1. The shape of chamber was cylinder. To prevent oxidation, the chamber was sealed by glass substrate and was filled with nitrogen gas. A suction nozzle was attached to the chamber for avoiding the accumulating fume. The laser beam was scanned in a straight line at spot size of approximately φ 30 μm and the scanned speed was controlled from 10 to 400 mm/s by galvanometer optical scanner. The areas were processed to a width of 3×6 mm^2 or 6×6 mm^2 under the condition of line pitch of 12.5 μm as shown in Fig. 1.

2.2 Optical properties and the structure of blackened surface

Figure 2 shows the result of laser pulse ablation for each scanning speed. The surface color darkens as the scan speed decreases. Above 150 mm/s rate, there is no difference in appearance. To confirm that an oxidation of surface is small, we measured a weight concentration of each surfaces using SEM–EDS (Energy Dispersive X-ray Spectroscopy). The oxygen spectra of the processed surfaces were within 0.5–1.85 times the non-processed surface. On the other hand, the oxygen spectra of surfaces processed in non-purge condition were 2.3–6.7 times the non-processed surface. A relative reflectivity of processed area was measured by spectrophotometer (SolidSpec-3700 UV–VIS-NIR SPECTROPHOTOMETER, Shimazu Corp.) as shown in Fig. 3. The data were normalized by the reflectivity of the non-processed substrate.

To gain a deeper understanding of blackened surface, we observed the surface by SEM. Figure 4 shows the SEM images of the surfaces blackened at three different scan rate. The upper figures show the surface image and the lower figures show the cross section image. The image shows the nano-particles condensing to form grape-like masses the size of few micrometer. Also, the number of nano-particles is increasing as the scan speed decreases. At a slow scan speed of 10 mm/s, a condensed structure with depth above 100 μm and aspect ratio above 1:10 can be seen in Fig. 4d. Such dense fractal structure in the range of nanometers to micrometers is known to create effective light trapping [11, 14, 17].

The experiment was also carried out using sub-nanosecond pulsed laser with pulse duration of 370 ps. We could not obtain the light-absorbing fractal structures in nitrogen-purge condition. In case of non-purged condition, surface was slightly darkened as in Fig. 2c–f, but by oxidation instead of formation of nano-structures.

3 Scattering and absorption efficiency calculated by Mie scattering theory

We theoretically investigated the light-absorbing nanostructure using 3D FDTD. To optimize the calculation efficiency, we first estimated the effect of nano-particles on surface reflectivity using Mie scattering theory. The following equations are available to calculate the scattering cross section C_{sca} [18, 19]:

$$C_{sca} = \frac{2\pi}{k^2}\sum_{n=1}^{\infty}(2n+1)\left(|a_n|^2+|b_n|^2\right), \tag{1}$$

where a_n and b_n are Mie scattering coefficients and k is wavenumber. The absorption cross section C_{abs} is derived from following equations,

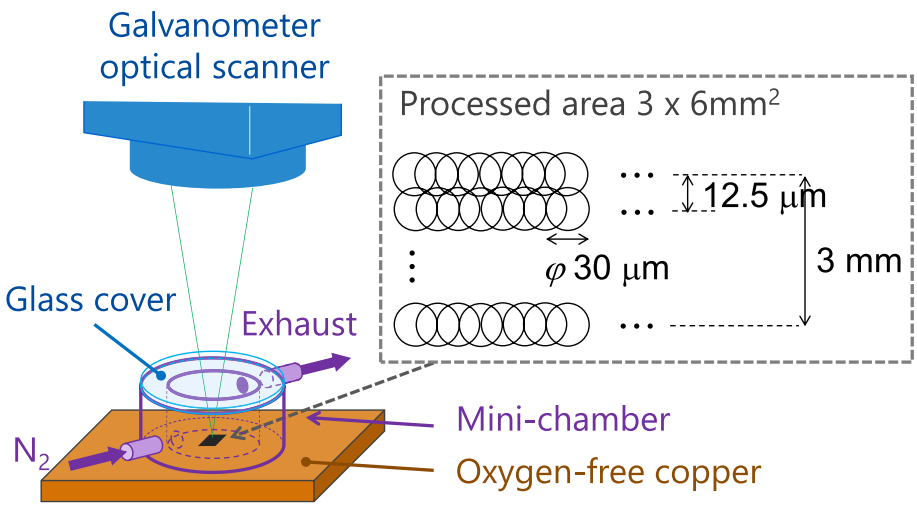

Fig. 1 Experimental setup for the surface blackening of copper. A suction nozzle was attached to the side of the chamber to avoid the accumulating fume. The laser beam was scanned in a straight line at spot size of approximately φ 30 μm. The scan speed was controlled from 10 to 400 mm/s by galvanometer optical scanner. The areas were processed to a width of 3×6 mm^2 or 6×6 mm^2 the 12.5 μm pitch

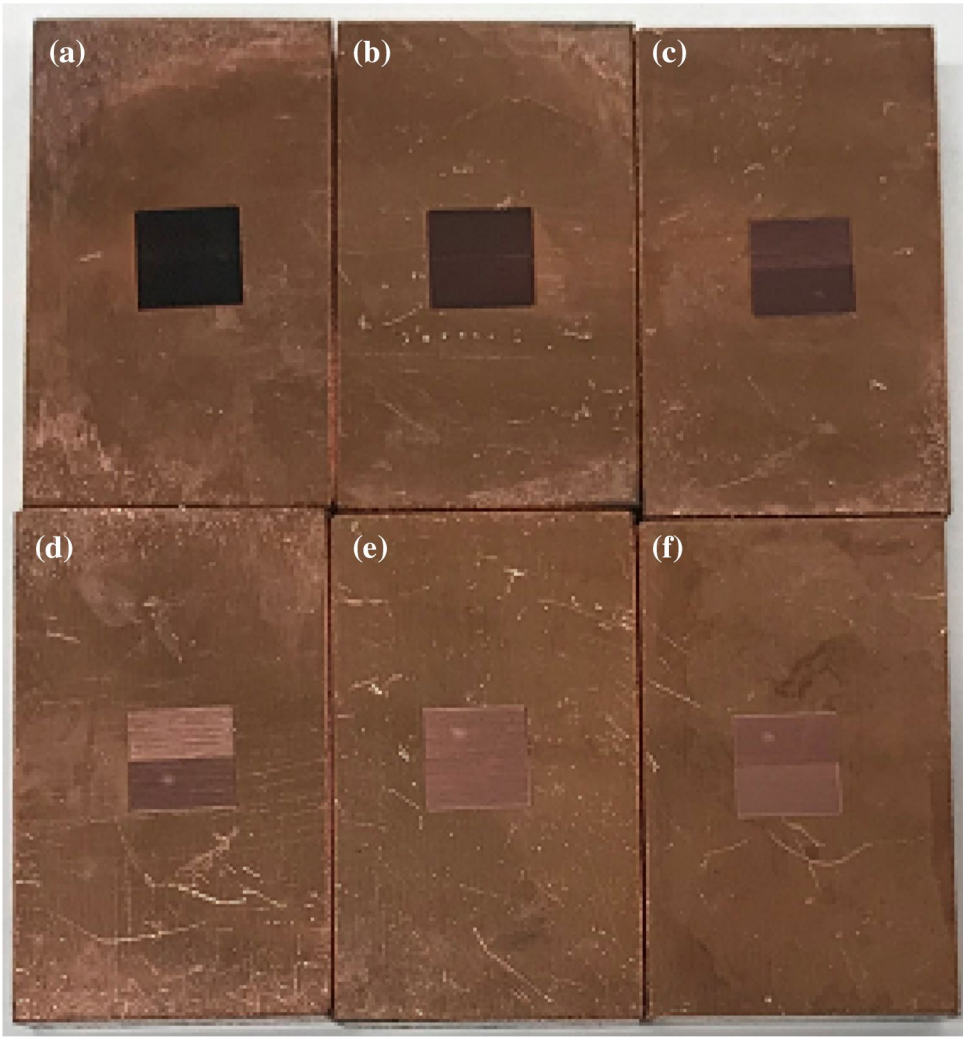

Fig. 2 Microscope photograph of darkened area processed by scan speeds of **a** 10 mm/s, **b** 50 mm/s, **c** 100 mm/s, **d** 150 mm/s, **e** 200 mm/s, **f** 400 mm/s

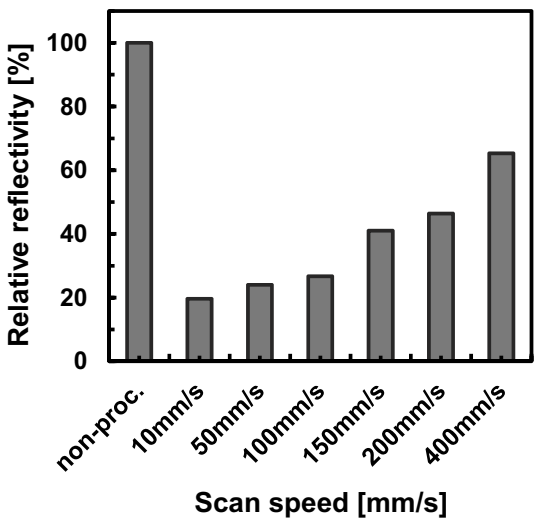

Fig. 3 Dependence of the relative reflectivity on the scan speed. Each measured data were normalized by the reflectivity of non-processed substrate

$$C_{\text{ext}} = \frac{2\pi}{k^2}\sum_{n=1}^{\infty}(2n+1)\text{Re}\left(a_{\text{n}} + b_{\text{n}}\right), \tag{2}$$

$$C_{\text{sca}} = C_{\text{ext}} - C_{\text{abs}}, \tag{3}$$

where C_{ext} is the extinction cross section. The scattering efficiency Q_{sca} and the absorption efficiency Q_{abs} are derived from the Eqs. (1) and (3) divided by particle cross section ($2\pi r^2$).

Figure 5 shows the dependence of the scattering and absorption efficiency on the particle diameter for the wavelength of laser welding ($\lambda = 1030$ nm). The optical properties of copper are $n = 0.26039$ and $k = 6.7001$ [20]. The result shows that the absorption efficiency is negligibly small compared with scattering efficiency for particles less than 2 μm. Hence, the surface blackening is not an absorption phenomena, but a light trapping by multiple scattering inside the fractal nano-structure. For determining the calculation condition of the small particle's size range in FDTD model, we

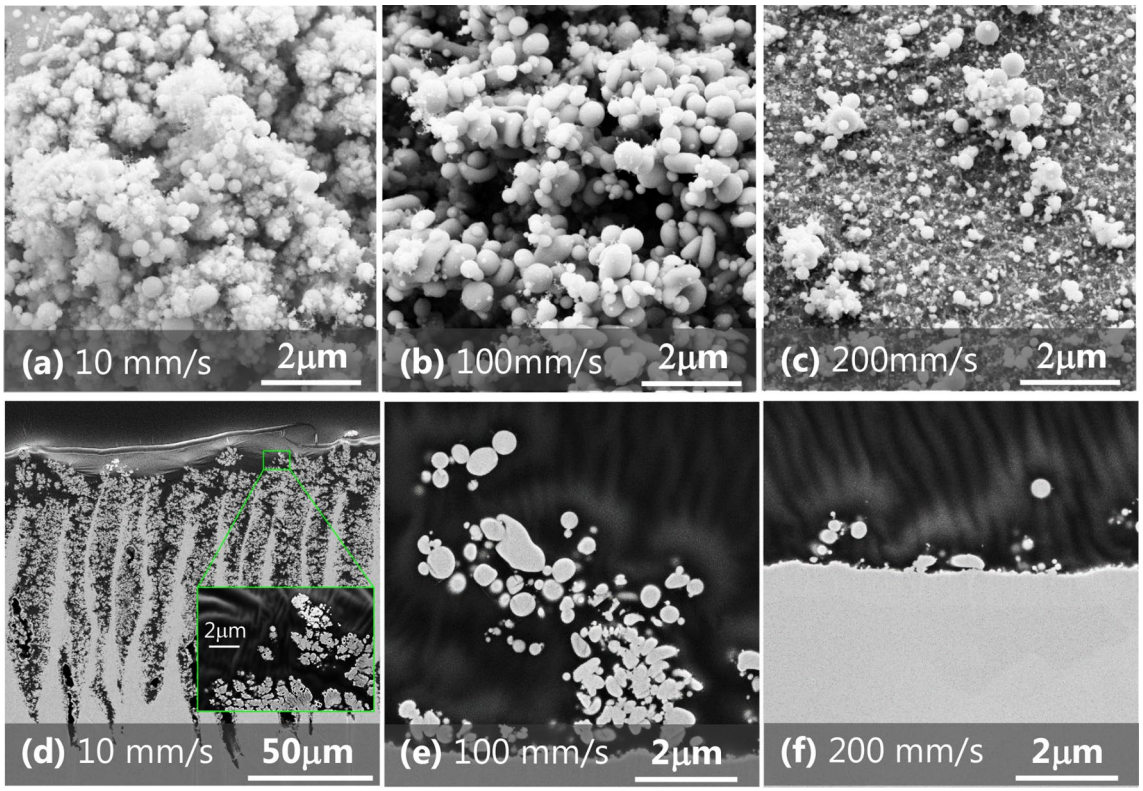

Fig. 4 SEM images of three types of nano-structure fabricated by picosecond laser irradiation on the copper surface. The upper figures show the surface image and the lower figures show the cross section image. The scan speed is described in each figures

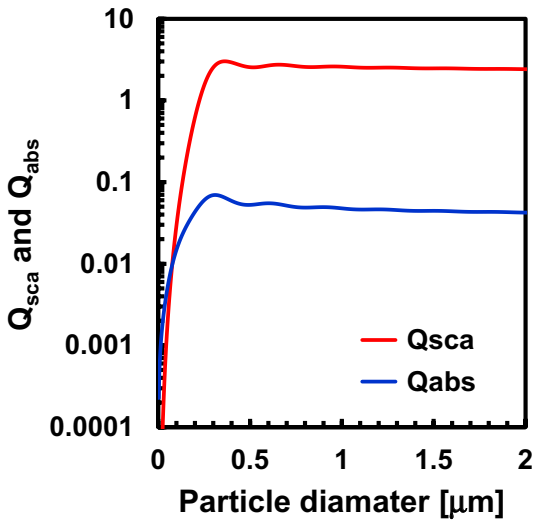

Fig. 5 Dependence of the scattering and absorption efficiency on the particle diameter. Both efficiencies, Q_{sca} and Q_{abs}, are calculated at wavelength of 1030 nm

also studied the interaction of the size effect. Figure 5 shows that both curves drop precipitously for particles smaller than 400 nm. We, therefore, determined to only model particles larger than 400 nm in size.

4 Reflectivity calculation of nano-structure using 3D FDTD

4.1 Calculation model

We used the 3D FDTD method to calculate the reflectivity and the electric field distribution around nano-structure. This method, based on Maxwell's equations, is proven [21] to give an accurate distribution of the electromagnetic field in the near and far field in the structures with arbitrary shapes. Randomly placed small copper particles on copper substrate in vacuum environment were simulated. A diameter of particle size ranged from 0.4 to 2 μm. A computational domain was $20\times20\times50$ μm^3. The size of cell within the computational domain was 50 nm. A boundary condition of top and bottom of the domain was perfectly matched layer (PML), while the side wall of the domain was periodic condition. The electric field strength of the incident light was assumed as 1 V/m, and the light sources were placed at 49 μm height. To calculate reflectivity, power monitor was placed on the top of the domain, and five types of calculation model were used. One was a simple plane plate without particles. Other four models consisted of randomly placed nano-particles with 5 μm, 10 μm, 20 μm, and 40 μm height, as shown in Fig. 6.

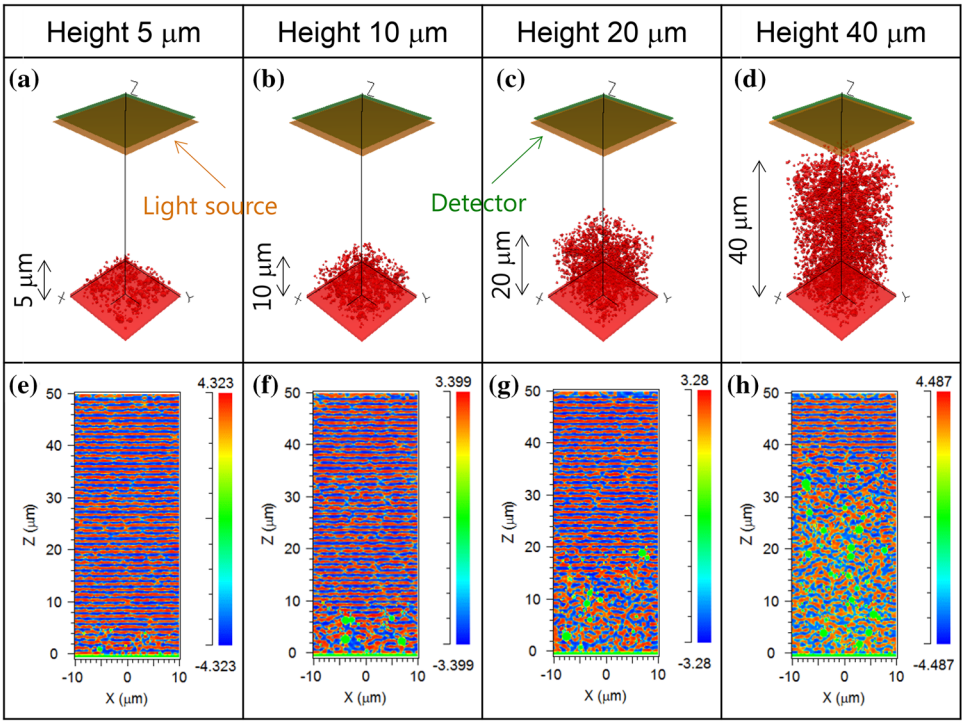

Fig. 6 **a**–**d** Four types of calculation model consisting of nanoparticles. The computational domain is $10\times10\times$ m^3. The particles are distributed randomly on the copper plate. The particle size ranges 0.4–2.0 μm. The height of distributed range is 5 μm, 10 μm, 20 μm, and 40 μm, respectively. **e**–**h** Electric field distribution in a steady state (x–z plane, $y=0$ mm) calculated by 3D FDTD method. The incident wavelength is 1030 nm directed along the $-z$ direction. The polarization is parallel to the x-axis

4.2 Electric field distribution and reflectivity

Figure 6e–h shows the distribution of electric field in a steady state at the same time. Figure 7a shows the electric field distribution of 40 μm height model after 168 fs has elapsed. 168 fs is the time for electric filed to reach the plane plate at the bottom. Clearly, the penetrating speed into the nano-structure at its center is slow. Figure 7b shows the electric field distribution of 40 μm height model after 210 fs has elapsed. More light has penetrated into the nano-structure, but compared with Fig. 6h, it is still far from steady state. Figure 8 shows the reflectivity of each calculation models. The reflectivity is decreasing as the height of nano-structures increases. We conclude that the reflectivity depends on the height of the structure.

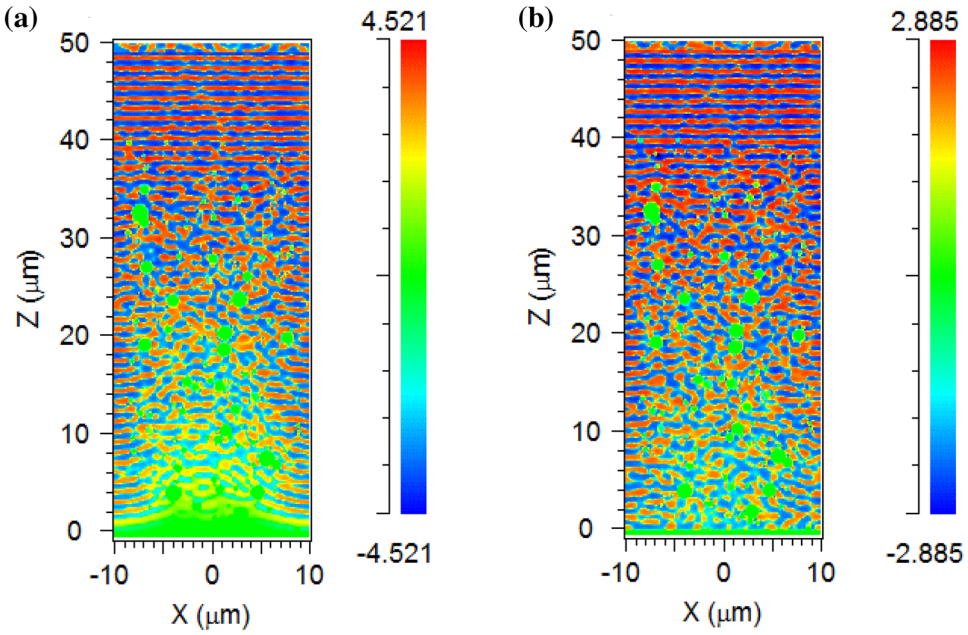

Fig. 7 Electric field distribution (x–z plane, $y=0$ mm) during scattering. **a** The distribution at 168 fs, **b** The distribution at 210 fs

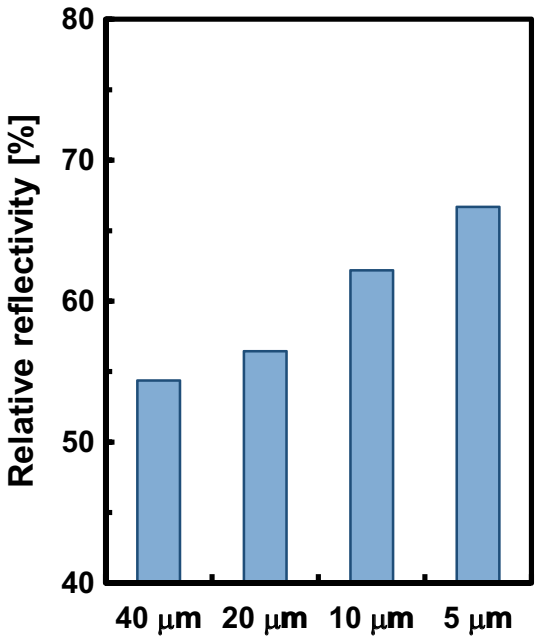

Fig. 8 Relative reflectivity of each calculation models. All calculated data are normalized by the reflectivity of non-processed copper plate

5 Effect of surface blackening on laser welding

We conducted a laser welding experiment using the blackened surface and non-processed surface. The laser welding was performed using a CW laser (Tru-Disk 4001, TRUMPF Inc.). The laser output at center wavelength of 1030 nm with maximum power of 4 kW. The laser beam was delivered by optical multimode fiber with a core size of 0.1 mm. The delivered beam was focused by optical system with 2.3 times magnification and scanned for 40 mm in a straight line at the spot size of φ 0.23 mm and scan speed of 300 mm/s by galvanometer optical scanner. The processing area was purged with nitrogen gas by a spraying nozzle.

Figure 9 shows the microscope images after laser welding. The figure on the left side shows welding to non-processed copper surface and the figure on the right side shows welding to blackened copper surface fabricated by the scan speed of 10 mm/s.

The power threshold in laser welding on the non-processed and the blackened copper surface is 3250 W and 1000 W, respectively. The difference of the threshold is three times. Furthermore, in comparing the bead width on two surfaces at 3500 W, the bead width on normal surface is unstable, while that on the blackened surface is stable. Obviously, the

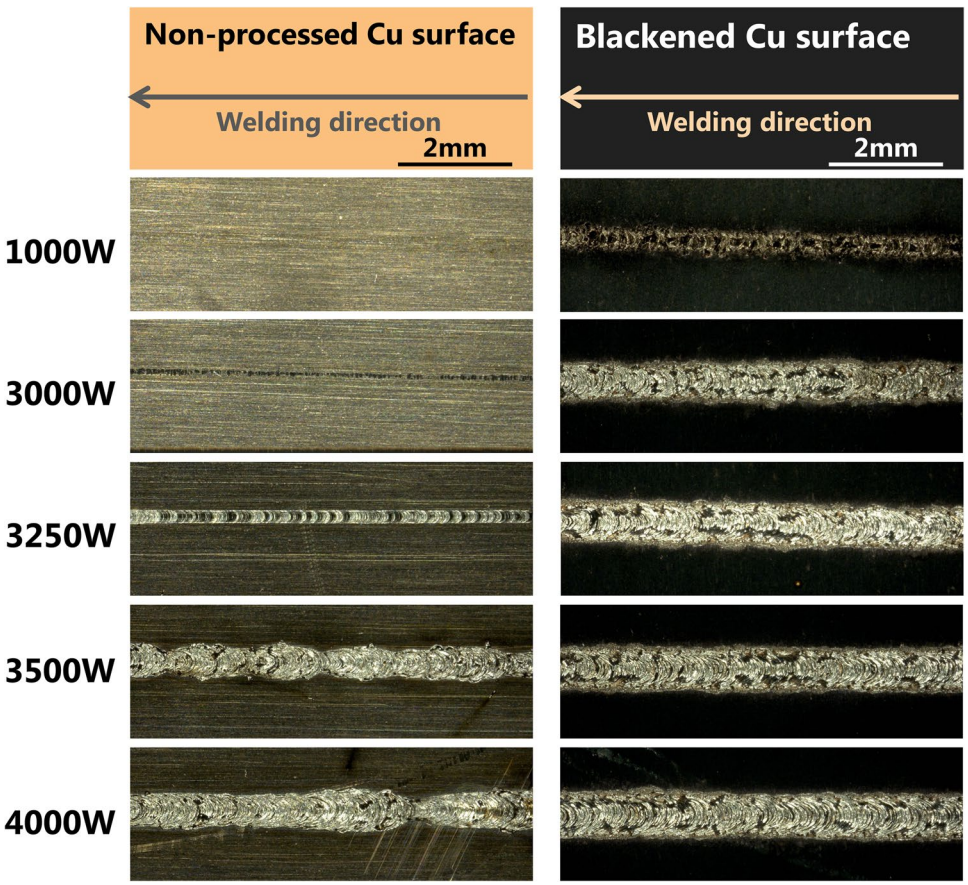

Fig. 9 Microscope images after CW laser welding with wavelength of 1030 nm. The spot size was 0.23 mm and the scan speed was 300 mm/s. The figure on the left side shows welding to non-processed copper surface and the figure on the right side shows welding to blackened copper surface fabricated by the scanning speed of 10 mm/s

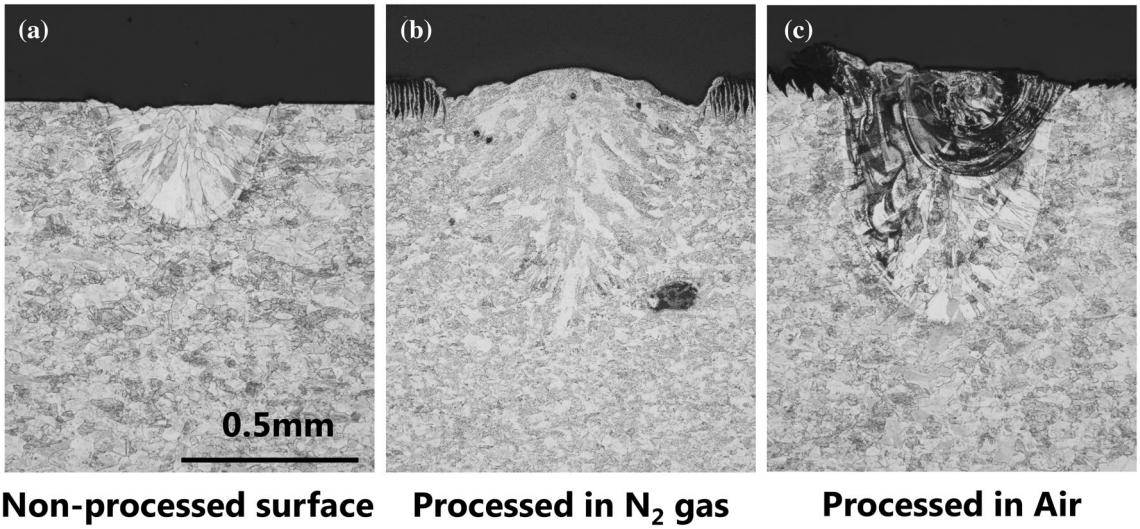

Fig. 10 Microscope images of cross section of the weld region. **a** Non-processed surface, **b** surface processed in N_2 and **c** surface processed in air

blackened surface has an effect on the decreasing threshold and being stable state of the bead. Figure 10 shows the cross section images of laser welding at 4000 W. The depth of welding in the blackened surface is two times deeper than that of non-processed surface as shown in Fig. 10a and b. Figure 10c shows the welded cross section when the surface was blackened without nitrogen gas. The analysis using EDS showed that the black-colored areas were all copper oxide, proving that surfaces blackened with nitrogen gas is not oxidized.

6 Conclusion

Decreasing of the reflectivity of copper was performed by nano-structure fabricated using picosecod laser pulses. The blackening was caused by multi-scattering due to the aggregated nano-particles. The scattering efficiency was calculated by Mie scattering theory, and the size of nano-particles above 0.4 µm was found to have strong scattering efficiency. The dependence of reflectivity on the height of the structure was numerically simulated using 3D FDTD method. The reflectivity decreased as the height of nano-structure increases. We applied this blackened surface to laser welding of copper. The threshold of laser welding on the blackened surface was three times lower than that of non-processed surface.

References

1. T. Gottwald, V. Kuhn, S.-S. Schad, C. Stolzenburg, A. Killi, Recent developments in high power thin disk lasers at TRUMPF laser. Proc. SPIE **8898**, 88980P (2013)
2. M.N. Zervas, C.A. Codemard, High power fiber lasers: a review. IEEE J. Sel. Top. Quantum Electron. **20**, 0904123 (2014)
3. H. Fritsche, F. Ferrario, R. Koch, B. Krusche, U. Pahl, S. Pflueger, A. Grohe, W. Gries, F. Eibl, S. Kohl, M. Dobler, Direct diode lasers and their advantages for materials processing and other applications. Proc. SPIE **9356**, 93560I (2015)
4. F. Schmitt, B. Mehlmann, J. Gedicke, A. Olowinsky, A. Gillner, R. Poprawe, Laser beam micro welding with high brilliant fiber lasers. J. Laser Micro/Nanoeng. **5**, 197 (2010)
5. A. Das, D. Li, D. Williams, D. Greenwood, Joining technologies for automotive battery systems manufacturing. World Electric. Veh. J. **9**, 22 (2018)
6. A. Heider, P. Stritt, A. Hess, R. Weber, T. Graf, Process stabilization at welding copper by laser power modulation. Phys. Procedia **12**, 81 (2011)
7. A. Hess, R. Schuster, A. Heider, R. Weber, T. Graf, Continuous wave laser welding of copper with combined beams at wavelength of 1030 nm and of 515 nm. Phys. Procedia **12**, 88 (2011)
8. S. Engler, R. Ramsayer, R. Poprawe, Process studies on laser welding of copper with brilliant green and infrared lasers. Phys. Procedia **12**, 339 (2011)
9. A. Balck, M. Baumann, J. Malchus, R.V. Chacko, S. Marfels, U. Witte, D. Dinakaran, S. Ocylok, M. Weinbach, C. Bachert, A. Kösters, V. Krause, H. König, A. Lell, B. Stojetz, A. Löffler, U. Strauss, 700W blue fiber-coupled diode-laser emitting at 450 nm. Proc. SPIE **10514**, 1051403 (2018)
10. C. Wu, C.H. Crouch, L. Zhao, J.E. Carey, R. Younkin, J.A. Levinson, E. Mazur, R.M. Farrell, P. Gothoskar, A. Karger, Near-unity below-band-gap absorption by microstructured silicon. Appl. Phys. Lett. **78**, 1850 (2001)
11. A.Y. Vorobyev, C. Guo, Direct femtosecond laser surface nano/microstructuring and its applications. Laser Photonics Rev. **7**, 385 (2013)
12. A.Y. Vorobyev, C. Guo, Spectral and polarization responses of femtosecond laser-induced periodic surface structures on metals. J. Appl. Phys. **103**, 043513 (2008)
13. A.Y. Vorobyev, C. Guo, Femtosecond laser blackening of platinum. J. Appl. Phys. **104**, 053516 (2008)
14. H. Huang, L.-M. Yang, S. Bai, J. Liu, Blackening of metals using femtosecond fiber laser. Appl. Opt. **54**, 324 (2015)

15. P. Fan, M. Zhong, L. Li, T. Huang, H. Zhang, Rapid fabrication of surface micro/nano structures with enhanced broadband absorption on Cu by picosecond laser. Opt. Express **21**, 11628 (2013)
16. Z. Huang, J.E. Carey, M. Liu, X. Guo, E. Mazur, J.C. Campbell, Microstructured silicon photodetector. Appl. Phys. Lett. **89**, 033506 (2006)
17. T.-H. Her, R.J. Finlay, C. Wu, S. Deliwala, E. Mazur, Microstructuring of silicon with femtosecond laser pulses. Appl. Phys. Lett. **73**, 1673–1675 (1998)
18. G. Mie, Ann. Phys. (Leipz.) **25**, 377 (1908)
19. C.F. Bohren, D.R. Huffman, *Absorption and scattering of light by small particles* (Wiley-VCH, Weinheim, 1983)
20. A.D. Rakic, A.B. Djurisic, J.M. Elazar, M.L. Majewski, Optical properties of metallic films for vertical-cavity optoelectronic devices. Appl. Opt. **37**, 5272 (1998)
21. A. Taflove, S.C. Hagness, *Computational electrodynamics: the finite-difference time-domain method* (Artech House, Boston, 2000)